Food Chemistry: X 24 (2024) 101841

Contents lists available at ScienceDirect

Food Chemistry: X

journal homepage: www.sciencedirect.com/journal/food-chemistry-x

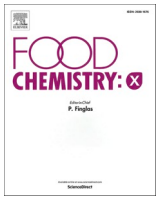

pH-induced interface protein structure changes to adjust the stability of tilapia protein isolate emulsion prepared by high-pressure homogenization

Qingguan Liu, Ailin Chen, Pengzhi Hong, Chunxia Zhou *, Xiang Li, Mengya Xie

College of Food Science and Technology, Guangdong Ocean University, Zhanjiang 524088, China

ARTICLE INFO

Keywords:
Tilapia protein isolate
pH
Secondary structure
Emulsion stability
Correlation analysis

ABSTRACT

The pH is a crucial external factor affecting the structure and emulsification characteristics of proteins. The current study aimed to reveal the correlation between the secondary structure changes and tilapia protein isolate (TPI) emulsion stability under different pH (3.0–10.0) prepared by high-pressure homogenization. The results showed that TPI with significantly increased solubility and emulsifying properties when the pH keep away from the isoelectric point (pH 5.0). Meanwhile, TPI emulsions presented significantly enhanced stability (with decreased particle size, increased zeta potential, creaming index close to 0, and uniform dispersion of droplets) at pH 3.0 and 10.0. Interface-adsorbed protein mainly consists of a myosin-heavy chain and actin, and the secondary structure was significantly influenced by pH and high-pressure homogenization. The α-helix will be transformed into β-sheet and β-turn when pH is closer to pH 5.0. However, the high-pressure homogenization induced α-helix conversion to β-sheet. The correlation analysis revealed that emulsion stability is positively correlated with α-helix and negatively correlated with β-sheet. This work provides a deep insight into the correlation between secondary structure changes and the stability of TPI emulsion as affected by pH to offer an alternative way to enhance TPI emulsion stability.

1. Introduction

Nile tilapia is a common freshwater fish in the aquaculture industry, and the world's aquaculture production was about 7.0 million tons in 2024 (FAO, 2024). Tilapia muscles have high-quality protein, higher protein digestibility, and less pressure on the environment (Egerton, Culloty, Whooley, Stanton, & Ross, 2018; Van, Keuchenius, De, De, & Aiking, 2018). At present, tilapia is usually processed into frozen tilapia fillets and surimi products. In recent years, tilapia muscle has been used to extract tilapia protein isolate (TPI) as a potential substitute for animal and plant proteins due to its advantages such as easy availability, high nutritional value, and sustainability compared to protein sourced from other freshwater fish (Tan et al., 2019; Xie et al., 2024). Based on these advantages, TPI has been used to prepare dual protein systems (Li et al., 2024; Li, True, Sha, & Xiong, 2024; Liu, Tan, Hong, Liu, & Zhou, 2024) and gel products (Huang et al., 2024). However, reports on the preparation of protein-based emulsions using TPI are relatively scarce. Therefore, studying the emulsifying properties of TPI is of significant scientific importance for expanding its applications in food-based emulsion products.

Protein can form a single molecular layer on the interface of two heterogeneous solutions to generate a uniform and stable dispersion system. Protein emulsifiers commonly used in processed food mainly include whey protein (Liu, Sun, Cheng, Zhang, & Guo, 2022) and plant protein (Hu et al., 2023; Zhang et al., 2022; Zhang et al., 2022). Indeed, potential applications of aquatic proteins have received increasing attention, such as hairtail protein (Huang et al., 2023), sea bass protein (Wu et al., 2024), and cod protein (Ma et al., 2020). The study reported that fish protein is a potential inhibitor for emulsion phase separation and lipid oxidation (Chalamaiah, Kumar, Hemalatha, & Jyothirmayi, 2012). However, limited research has been done on the TPI emulsifying properties and emulsion development due to its poor solubility. Researchers found that cod protein can be effectively modified by ultrasonic treatment and high-pressure homogenization to serve as an emulsifier (Ma et al., 2019; Ma et al., 2020). Therefore, appropriately modifying tilapia protein may be applied as a stabilizer for developing stable oil-in-water (O/W) emulsions.

Protein emulsification is susceptible to many factors (Xia, Kong, Xiong, & Ren, 2010). Among all factors, pH is the most important external factor affecting protein structure and functional properties. In

* Corresponding author.
E-mail address: chunxia.zhou@163.com (C. Zhou).

https://doi.org/10.1016/j.fochx.2024.101841
Received 24 April 2024; Received in revised form 20 August 2024; Accepted 16 September 2024
Available online 17 September 2024

general, the partial unfolding of protein can enhance the solubility and emulsification of globular proteins under extreme pH environments (Jiang, Chen, & Xiong, 2009; Tian, Zhang, Zhang, Taha, & Pan, 2020). The combination of homogenization pretreatment and alkaline treatment (pH 10.0 and 12.0) can enhance the interfacial properties and emulsification characteristics of soy peptide aggregates (Du et al., 2020). Threadfin bream stabilized emulsion prevents flocculation by hydrophobic interaction at pH 12.0 (Felix, Romero, & Guerrero, 2017; Hemung, Benjakul, & Yongsawatdigul, 2013). Research has shown that protein flexibility is related to functional properties. Flexible protein is susceptible to denaturation at the interface and exhibits good emulsifying and foaming properties (Kato, Komatsu, Fujimoto, & Kobayashi, 1985). The changes in pH will expose the charged groups of proteins and change the secondary structure and flexibility, which promote protein rearrangement and adsorption onto the O/W interface to improve emulsion stability (Xi et al., 2020; Yan, Xu, Zhang, & Li, 2021). Therefore, we hypothesized that pH coupled with high-pressure homogenization treatment may affect the structure and surface properties of TPI, thus improving the emulsion stability.

This study aimed to investigate the characteristics and stability of TPI emulsion under different pH (3.0–10.0) prepared by high-pressure homogenization treatment. Solubility and emulsification characteristics of TPI, stability and microstructure of emulsion, structure and composition of TPI in O/W interface were investigated. The correlation between TPI secondary structure changes and emulsion stability was revealed.

2. Materials and methods

2.1. Materials

Fresh Nile tilapia meat was obtained from the local aquatic market (Zhanjiang, Guangdong province, China) for immediate use or frozen at −20 °C no more than 5 days. Corn oil was procured from Wal-Mart (Zhanjiang, China). Nile Red and Nile Blue were purchased from Solebold (Beijing, China). All other reagents were of analytical grade.

2.2. Extraction of TPI

TPI was extracted from the method of Al-Saadi and Deeth (2011), with some modifications. Tilapia meat was chopped and blended with distilled water with the proportion of 1:9 (*w/v*) and then homogenized (10,000 rpm, 2 min) by a high-speed homogenizer (T-18, IKA, Germany). The homogenate's pH was shifted to 11.0 by NaOH (1.0 M) and stirred at 450 rpm for 30 min. The stirred protein solution was centrifuged (10,000*g*, 20 min) by a centrifuge (J-26sxp, Avanti, Beckman, USA). The supernatant's pH was adjusted to 5.5 using 1.0 M HCl and then centrifuged (10,000*g*, 20 min). Acquired precipitates were resuspended by deionized water and adjusted to pH 7.0. The pH-adjusted protein was dialysised using dialysis bags (8000–14,000 Da) for 48 h and then lyophilized and stored at −20 °C for backup. The obtained TPI powder had protein contents of 96.05 ± 0.764 % (N × 6.25), which was detected by a Kjeldahl nitrogen analyzer (K1100, Haineng, China).

2.3. Protein solubility of TPI

Protein solubility under different pH was determined based on a previous method (Kristinsson & Hultin, 2004) with minor modifications. TPI dispersions (5 mg/mL) were shifted to different pH (3−10) after 30 min. The pH-adjusted TPI solutions were centrifuged (10,000*g*, 20 min). The supernatant was collected for detecting protein content based on the Lowry method. Absorbance in 750 nm was measured by an ultraviolet spectrophotometer (Cintra 1010, GBC Scientific Equipment Pty., Ltd., Australia), and sample solubility was calculated by the formula below:

$$\text{Protein solubility}(\%) = \frac{\textit{Supernatant protein content}}{\textit{Protein content before centrifugation}} \times 100 \quad (1)$$

2.4. Emulsifying activity index (EAI) and emulsifying stability index (ESI) of TPI

The EAI and ESI of TPI under pH 3.0–10.0 were detected using a method (Pearce & Kinsella, 1978). The 6 mL TPI solution (5 mg/mL) was mixed with corn oil (2 mL) in a 50 mL measuring cup and homogenized (12,000 rpm, 1 min) by a homogenizer. The emulsion from the bottom (20 μL) was blended with 0.1 % sodium dodecyl sulfate solution (4 mL). Sample absorbance at 500 nm was determined by an ultraviolet spectrophotometer at 0 min (A_0) and 10 min (A_{10}). The calculation equations are as follows:

$$\text{EAI}\ (m^2/g) = \frac{2 \times 2.303 \times A_0 \times DF}{C \times \Theta \times \varphi \times 10000} \quad (2)$$

$$\text{ESI}(min) = \frac{A_0}{A_0 - A_{10}} \times 10 \quad (3)$$

where *DF* is the dilution ratio (200), *C* represents protein concentration (g/mL), θ represents the oil volume fraction (0.25), and φ is the thickness of the cuvette (1 cm).

2.5. Preparation of TPI emulsion

Protein concentration was fixed at 10 mg/mL, and then pH was adjusted to a different range (3.0–10.0). The pH-adjusted protein solution was stirred by magnetic stirring under the ice water bath for 30 min. The protein phase was blended with oil phase at a volume ratio of 9:1 using a T-18 homogenizer (12,000 rpm, 2 min). The crude emulsions were homogenized (60 MPa, 4 °C) at five passes by a high-pressure homogenizer (APV-1000, Germany). The NaN_3 was added to the resulting emulsion to a final concentration of 0.02 % (*w/v*) as an antibacterial agent.

2.6. Characterization of TPI emulsion

2.6.1. Particle size and zeta potential

Samples were diluted 300-fold to avoid multiple light scattering. The particle size and zeta potential were detected by the NanoBrook Omni (Brook Haven Instruments, USA) at 25 °C. The emulsion stability was detected by droplet size changes over 28 days of storage (4 °C).

2.6.2. Stability coefficient

The stability coefficient of TPI emulsion with different pH treatments was detected using the method of Li et al. (2019). Ten milliliters of emulsions were centrifuged (3000*g*, 15 min). The original sample and the supernatant were diluted 100 times with distilled water. The absorbance at 375 nm was detected. The stability coefficient was calculated using the following equation:

$$\text{R}(\%) = \frac{A_1}{A_2} \times 100 \quad (4)$$

where R is the stability coefficient. A_1 and A_2 are the absorbance of the original sample and the supernatant after centrifugation.

2.6.3. Creaming index (CI)

The CI of varying samples was measured using the method of Surh, Decker, and McClements (2006) with some modifications. The emulsions were put into a 50 mL glass bottle and stored at 4 °C. The height of the serum (H_s) and total height (H_t) of the emulsions were detected during 28 days. The calculation equation of CI is as follows:

$$CI(\%) = \frac{H_S}{H_t} \times 100 \quad (5)$$

where H_s represents the serum phase height, and H_t represents the sample height.

2.6.4. Confocal laser scanning microscopy (CLSM)

TPI emulsions were diluted 20-fold and mixed with a mixture of dyes (0.01 % Nile red and 0.1 % Nile Blue dye in isopropanol). The dyed sample was kept in a dark room for 30 min, and then 10 μL of the sample was dripped onto the glass slide with a cover slip. Fluorescence images were obtained by a CLSM (Olympus FV3000, Ltd., Japan): 10× eye lens and 100× oil immersion lens at 488 nm (Argon laser) and 633 nm (Helium-Neon laser).

2.7. Structure and composition of TPI in O/W interface

2.7.1. Circular dichroism (CD) spectra

The secondary structure of TPI in the emulsion system was measured using a circular dichroism spectrometer (model J-810, Jasco, Japan) based on a previous method (Mozafarpour, Koocheki, Milani, & Varidi, 2019). Emulsions at different pH were diluted by distilled water to the protein concentration of 0.5 mg/mL. Samples were scanned in the wavelength range of 190–260 nm at a temperature of 25 °C. The scanning speed was set to 50 nm/min, with a response time of 0.5 s and a bandwidth of 1 nm.

2.7.2. Content of interface adsorbed protein

Interface adsorbed protein was determined according to the method of Ma et al. (2020). Fresh TPI emulsions at different pH (30 mL) were centrifuged (10,000*g*, 30 min, 4 °C) to separate an upper emulsified layer and a lower aqueous phase. The lower aqueous phase was aspirated by a syringe and filtered through a 0.45 μm filter. The unabsorbed protein content in the filtrate was detected using the Lowry method. Interfacial adsorbed protein percentage was calculated as follows:

$$F_{abs}(\%) = \frac{C_i - C_{ep}}{C_i} \times 100 \quad (6)$$

where C_i is the total protein concentration (kg/m^3), C_{ep} is the unabsorbed protein concentration (kg/m^3), and F_{abs} is the percentage of interfacial adsorbed protein.

2.7.3. Sodium dodecyl sulfate-polyacrylamide gel electrophoresis (SDS-PAGE)

The composition of interface-adsorbed protein and non-absorbed protein was determined through SDS-PAGE (Li et al., 2020). The emulsified layer after centrifugation was resuspended using NaCl buffer (0.6 M, 1:4, *v*/v) and then centrifuged at 10,000*g* for 30 min. This step was replicated three times for adequate removal of unadsorbed protein. Then, the emulsified layer was filtered with filter paper. The dehydrated emulsified layer and the aqueous phase were collected for the SDS-PAGE experiment by 12 % separating gel and 5 % stacking gel with a sample volume of 10 μL (Laemmli, 1970).

2.8. Statistical analysis

Data was repeated three times and expressed as mean ± standard deviations (Mean ± SD) unless specifically mentioned. Statistical differences between data were analyzed through one-way analysis of variance (AVONA) and Duncan's Multiple Range tests using SPSS 22.0, and $P < 0.05$ was identified as statistically significant.

3. Results and discussion

3.1. Solubility, EAI and ESI of TPI

The pH is the most important external factor affecting protein solubility and functional properties. Table S1 shows the influence of pH on TPI solubility, EAI, and ESI. The TPI solubility has a minimum value of pH 5.0 due to being near the protein isoelectric point (*pI*) (Brenner, Johannsson, & Nicolai, 2009). When the pH gradually deviated from 5.0, the solubility of TPI increased remarkably. The result agreed with the previous report that the *pI* of TPI was pH 5.5 (Brenner et al., 2009). The highest solubility (86.05 ± 2.41 %) was obtained at pH 10.0. Changes in pH can induce protein dissociation, unfolding, and rearrangement. High solubility at pH 3.0 and pH 10.0 suggested that the surface charge of protein may change, which is conducive to the enhancement of the intermolecular electrostatic repulsion. This change enhances ion-dipole interactions between the protein and water to resist the aggregation of proteins and provide more binding sites for water, thus improving the protein solubility (Wihodo & Moraru, 2013). TPI presented the maximum EAI and ESI at pH 10.0 and the minimum EAI and ESI at pH 5.0. Our results agreed with previous research that the deviation of pH from the *pI* of TPI induced the exposed hydrophobicity groups and free sulfhydryls, which may ultimately contribute to the increased emulsifying properties (Zhu, Li, Li, Ning, & Zhou, 2019). Additionally, the solubility of proteins is higher when they are far from their *pI*, which can promote the transfer of proteins to the oil-water interface (Liu et al., 2022), thereby enhancing their emulsifying properties. However, when close to the *pI*, the lower solubility of proteins will lead to protein aggregation or precipitation, which cannot fulfill the emulsification role (Xi et al., 2020).

3.2. Characterization of TPI emulsion

3.2.1. Particle size and zeta potential

Particle size is a crucial data for reflecting the emulsion stability. The size can influence the flocculation and aggregation of the emulsion (Li et al., 2019). The mean particle size of TPI emulsions reaches the lowest value at pH 3.0 and 10.0 (Fig. 1a insert), indicating that TPI formed smaller aggregates on the O/W interface when the pH was away from *pI*. Nevertheless, the largest particle size in micron level was found at pH 5.0, and the PDI value increased to 0.35 (Fig. 1a insert). This phenomenon was attributed to the decreased solubility of TPI at pH 5.0 (Table S1). The molecules quickly gather and form aggregates, which are adsorbed on the oil droplet surface to induce the increased emulsion particles.

Zeta potential was one of the most effective measures to evaluate the suspending liquid and emulsion in charge and the electrostatic interaction. The net surface charge of TPI emulsion was lowest at pH 5.0 due to approaching the protein *pI* (Fig. 1b). Emulsions have the largest net surface charge at pH 3.0 and 10.0 (Fig. 1b). The pH significantly affects protein interaction (flexible and charge), which led to some of the carboxyl groups, phenolic hydroxyl groups, and sulfhydryl groups buried in the protein ionize (Li et al., 2019). The high surface charge causes strong intramolecular electrostatic repulsion to maintain TPI emulsion stability. Interestingly, the absolute value of the zeta potential after high-pressure homogenization was greater than that of the crude emulsion without this treatment (Fig. 1b). This may be because high pressure disrupted the protein structure, leading to the exposure of some polar groups. Li, True, et al. (2024) also found that high-pressure treatment leads to an increase in the zeta potential of oat protein. The above results indicated that high-pressure homogenization and pH may affect protein structure and is beneficial to improve the emulsion stability. It will be further explained by the results of CD spectroscopy, as discussed later.

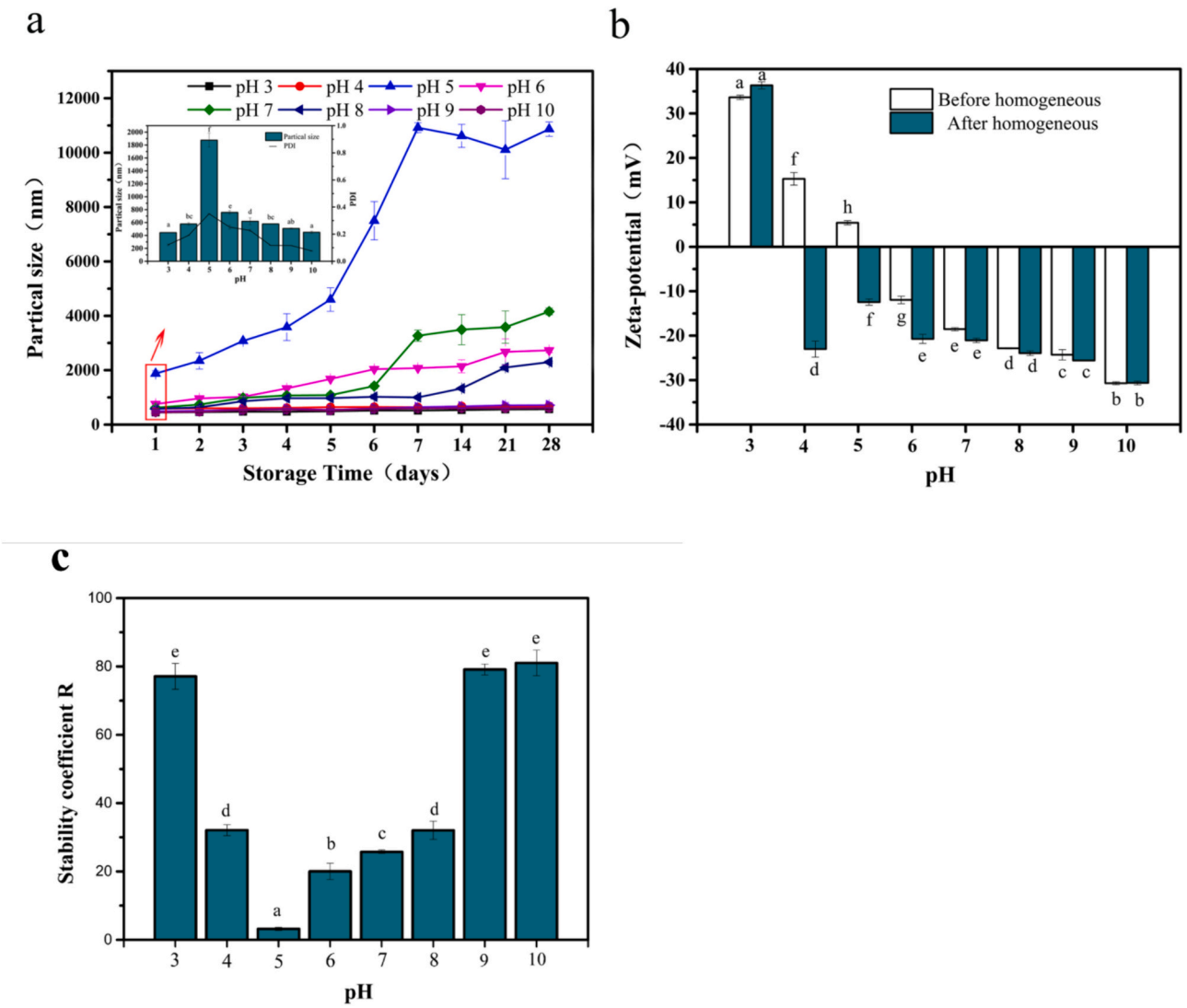

Fig. 1. Particle size and polydispersity Index (PDI) (a), zeta-potential (b), and stability coefficient (c) of TPI emulsions at different pH (3.0–10.0).

3.2.2. *Stability coefficient*

The stability coefficient (R) provides information on the settling rate and settling degree in the emulsion system to predict the long-term coalescence stability by centrifugation to accelerate droplet coalescence (Drapala, Mulvihill, & O'Mahony, 2018). The R-value was high (Fig. 1c) at pH 3.0, 9.0, and 10.0, indicating TPI emulsions were more stable. However, close to the *pI* of protein, the R values significantly decreased ($P < 0.05$) and has the minimum value at pH 5.0 (Fig. 1c), which agreed with data of zeta potential (Fig. 1b). Chen, Nicolai, Chassenieux, and Wang (2020) also found that the reduction of pH to the *pI* would reduce the charge density of proteins to reducing the strength of the repulsive interaction between proteins, thus facilitating their aggregation and stratification. The external environment (pH, pressure, and temperature) significantly influences protein interaction to result in changed emulsion stability (Garti, Slavin, & Aserin, 1999). Therefore, the pH value far from the *pI* will enhance the surface charge, and protein structure may change under electrostatic repulsion, thus improving emulsion stability.

3.2.3. *Creaming stability*

The CI and visual appearance are shown in Fig. 2. The emulsion at pH 5.0 with a CI value of more than 40 % showed an obvious phase separation. The emulsions showed gradually increased CI after 7 days of storage and phase separation at pH 6.0 and 7.0. However, emulsions remained stable during the 28 days of storage at pH 3.0, 4.0, 8.0, 9.0, and 10.0 (CI values were close to 0 and no significant phase separation). Changes in CI and visual appearance agreed with the particle size variations (Fig. 1a). The reason for this phenomenon is that less protein surface charge represented poor electrostatic repulsion between the molecules near the *pI* and enhanced the coalescence and aggregation of droplets (Yerramilli & Ghosh, 2017). However, under extreme acid-base conditions, the enhancement of surface charge is conducive to forming smaller aggregates and inhibition of phase separation. In addition, under extreme acid-base conditions, a large amount of TPI adsorbs at the oil-water interface, resulting in a reduction of interfacial free energy, which effectively resists gravity separation and aggregation to improve the storage stability of emulsions (Wang et al., 2024).

3.2.4. *CLSM*

Emulsion microstructure was observed by CLSM (Fig. 3). The result showed that almost all of the oil droplets presented globular and were trapped by protein molecules. Partial aggregation of TPI emulsions (relatively large and irregular emulsion droplets) was observed at pH 5.0 due to near the *pI* of TPI (Fig. 3a). Li et al. (2020) reported that the electrostatic repulsion between emulsions decreased when pH was close to the *pI* of soy protein, which promoted protein interaction and led to droplets aggregation. However, at lower and higher pH values (3.0 and 10.0), smaller sizes of TPI were easier to adsorb on the O/W interface,

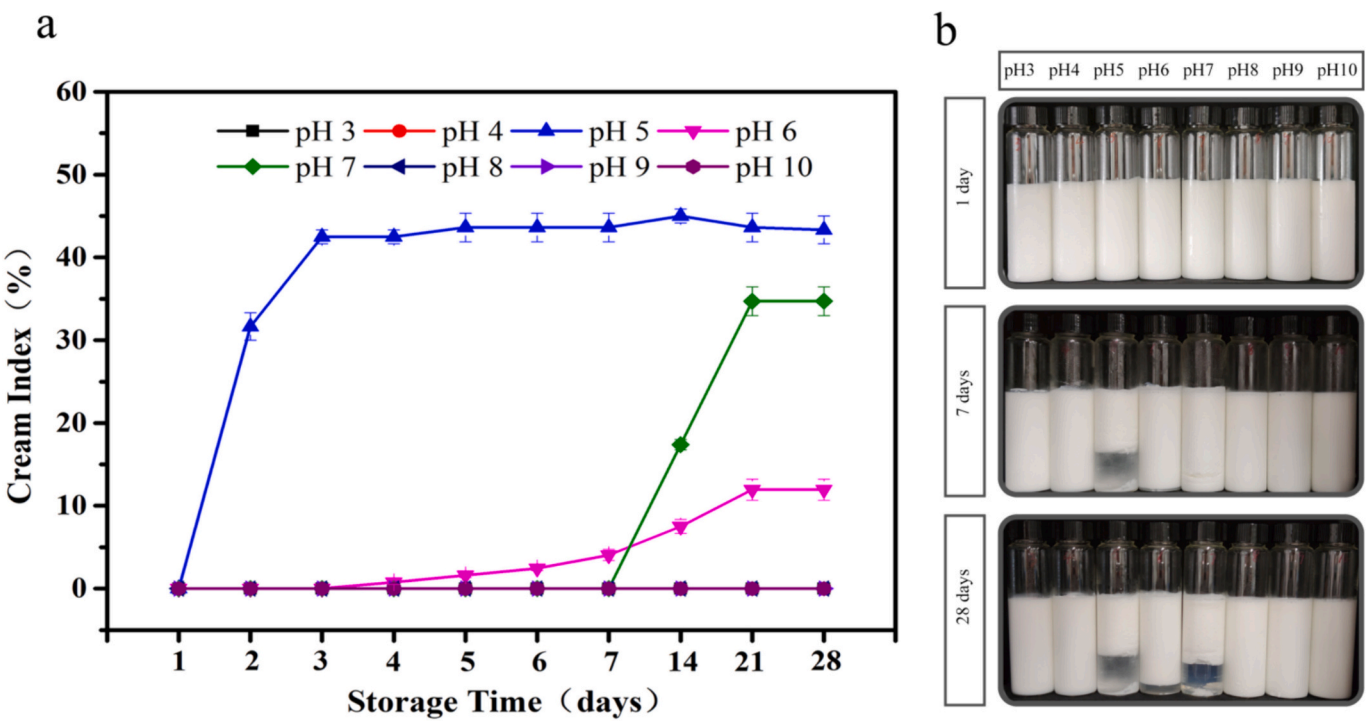

Fig. 2. Creaming index (CI) (a) and visual appearance (b) of TPI emulsions under different pH (3.0–10.0) at 4 °C storage for 28 days.

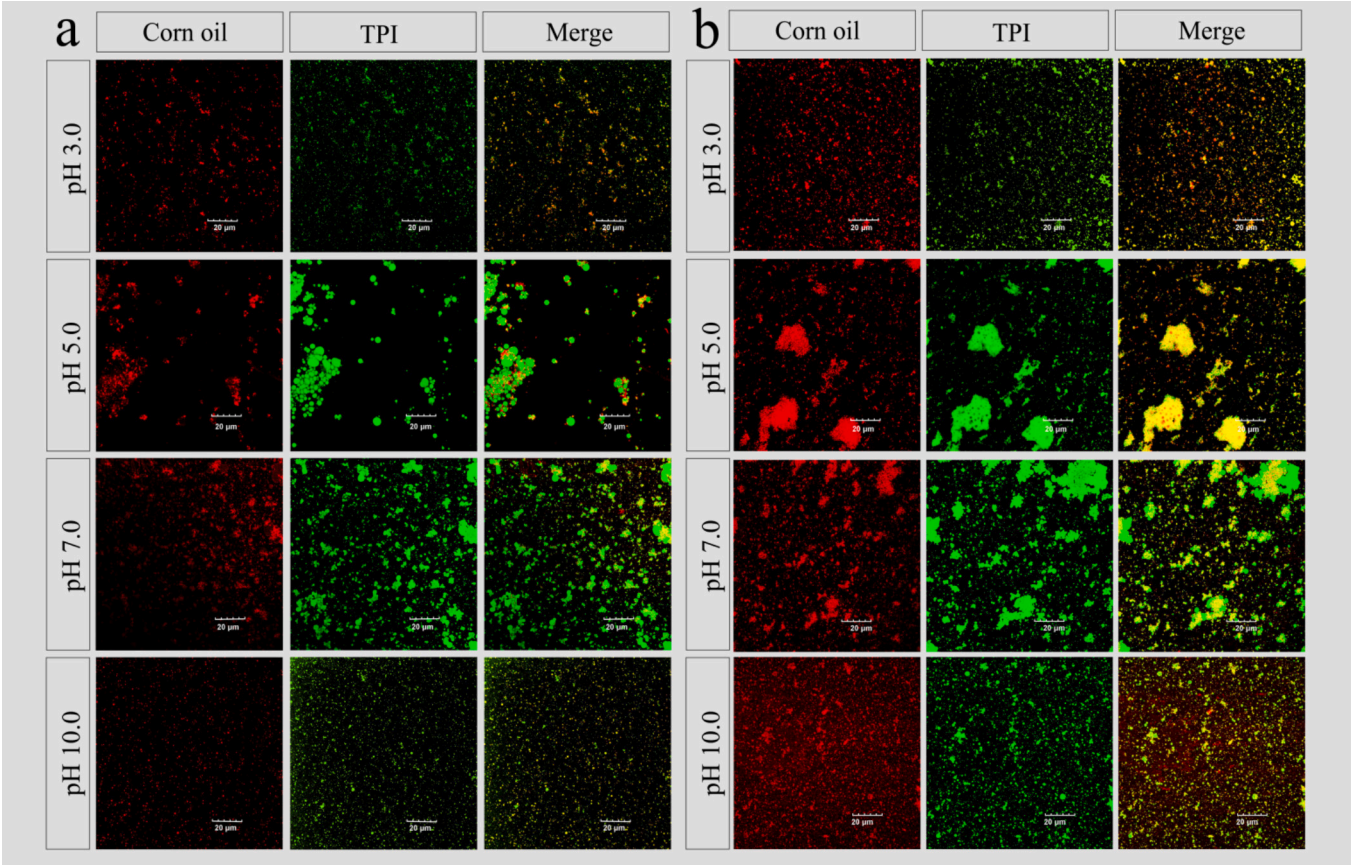

Fig. 3. CLSM images of TPI emulsions prepared by different pH (3.0–10.0) storage for 1 (a) and 7 (b) days.

resulting in uniform dispersion and stabilize of emulsions (Fig. 3a). Zhao, Bai, Xing, Xu, and Zhou (2018) have reported that decreased particle size and uniform dispersed droplets contributed to the stable emulsion system prepared by separated egg whites. Consistently, the decreasing particle size of emulsions at pH 10.0 and pH 3.0 (Fig. 1a) also confirmed this result.

The emulsion is a thermodynamically unstable system. Destabilization phenomena such as stratification, sedimentation, coalescence, and flocculation will occur, especially large droplets during storage. This phenomenon may be associated with secondary structure changes of protein in the emulsion system. After 7 days of storage, the stable emulsion with uniform morphologies preventing self-coalescence was detected at pH 3.0 and 10.0 (Fig. 3b). As for samples of pH 5.0 and 6.0, the aggregations of emulsions were observed (Fig. 3b), which due to pH close to the *pI* led to the decreased electrostatic repulsion. Away from the *pI*, the protein's secondary structure changes and improves protein solubility (Table S1). The smaller protein polymers formed a highly viscoelastic interfacial membrane on the droplet surface to prevent droplet aggregation via increased electrostatic repulsion (Fig. 1b). Therefore, it shows improved emulsion stability on a macro level with lower particle size (Fig. 1a) and CI value (Fig. 2a) during storage of 28 days. Zhang, Liu, et al. (2022) and Zhang, Zhou, et al. (2022) found that bamboo fungus protein gels (BGPs) stabilized emulsions have improved stability in alkaline environments, which might be attributed to the variation in electrostatic repulsion of BGPs. These results are consistent with our research.

3.3. Structure and composition of TPI in O/W interface

3.3.1. CD spectra

CD spectra are an excellent spectroscopic technique used to study the unfolding and folding of protein structures (Greenfield, 2006). The CD spectra and secondary structure content of TPI in the O/W interface were detected in the far ultraviolet range from 180 to 260 nm (Fig. 4 and Table 1). TPI in the O/W interface presented a positive spectral band near 192 nm and two negative spectral bands at 208 nm and 222 nm representing α-helix. The β-sheet showed a positive spectral band near 190 nm and a negative spectral band at 215 nm. The treatment of pH and high-pressure homogenization generated a significant influence on the CD spectra and secondary structure of the interfacial proteins.

When pH is closer to the *pI* of TPI, the content of α-helix decreases (16.77 ± 0.22 %), β-sheet and β-turn increase as high as 36.88 ± 0.66 % and 19.75 ± 0.37 (Table 1). With the increase of β-sheet, the protein polymerizes, causing the increased particle size of emulsions at pH 5.0 (Hu, Xie, Zhang, Li, & Qi, 2020). In addition, this case may also be attributed to the effect of pH on the hydrogen bonds inside the protein. After 60 MPa high-pressure homogenization treatment, the α-helix content reduced and part of α-helix conversion to β-sheet structures, especially in extreme acid and alkali conditions (Table 1). This phenomenon may be due to induced protein unfolding under homogenization pressure and conformational changes resulting from the disrupting hydrogen bonding and hydrophobic interactions (Hu et al., 2020). Secondary structure is related to protein aggregates, and high-pressure homogenization can destroy the original protein aggregates (Tomczynska-Mleko et al., 2014). In addition, consistent findings stated that the α-helix of water-soluble myofibrillar proteins (WSMP) decreased from 15.27 % to 13.23 % at homogenization of 10,000 psi (Chen, Zhou, Xu, Zhou, & Liu, 2017). Therefore, the conformation of the protein under the homogenization effect was changed, which promoted the extension of the protein's secondary structure and enhanced emulsion interface strength. The α-helix of emulsion at pH 3.0, 10.0 up to 44.67 ± 0.38, and 42.15 ± 0.99 respectively. Meanwhile, the emulsion presented improved stability. Therefore, we hypothesized that the α-helix content is positively correlated with the emulsion stability.

3.3.2. Content of interface adsorbed protein

Interface adsorbed protein content of TPI emulsion at pH 3.0–10.0 is shown in Fig. 5. TPI emulsions had the maximum adsorbed protein contents at pH 5.0 and 6.0, which may be due to the specificity properties of TPI: 65–80 % salt-soluble protein (such as myofibril) and 3–5 % water-insoluble protein. The protein near the *pI* has low solubility and will form water-insoluble aggregates to access oil droplets easily. The turbulence induced by high-pressure homogenization causes the higher aggregate to close to the surface of the oil droplets more quickly through convective mass transport in the turbulent flow fields (Nilsson & Bergenstahl, 2006). However, it should be emphasized that the emulsion stability is also related to interfacial film viscoelasticity. The protein at the interface layer is less unfolded to form aggregates when the pH is near the *pI*. Large protein aggregates with poorly hydrophilic hydrate can quickly close to the O/W interface and form a thick interface layer with poor elasticity. A stable emulsion cannot be formed due to the membrane because electrostatic repulsion between emulsion droplets is insufficient to prevent droplet aggregation. As moving away from the *pI*, smaller aggregates more slowly adsorbed to the surface of oil droplets than larger aggregates, resulting in low interfacial adsorption content. Langevin (2014) also found that the lower the interfacial adsorption protein content, the larger the interface space for protein structure unfolds. Once at the interface, a strong viscoelastic film can be formed, which provides sufficient electrostatic and spatial forces to generate a stable emulsion.

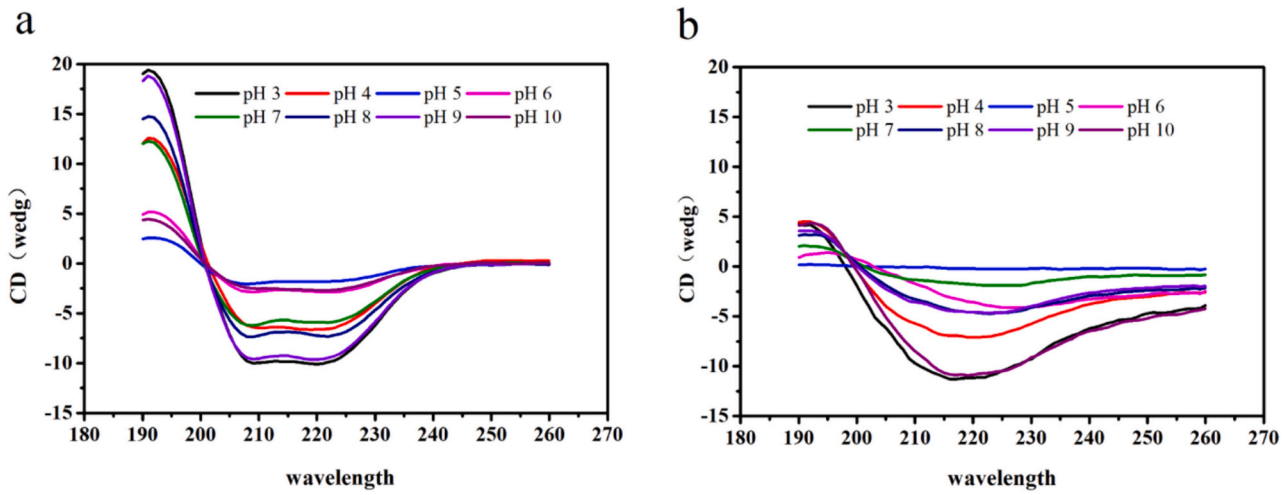

Fig. 4. CD spectra of TPI in emulsion systems before (a) and after (b) high-pressure homogenization at different pH (3.0–10.0).

Table 1
Effect of different pH on secondary structures (%) of TPI in in emulsion systems before and after homogenization.

pH	Before homogenization				After homogenization			
	α-helix (%)	β-sheet (%)	β-turn (%)	Random coil (%)	α-helix (%)	β-sheet (%)	β-turn (%)	Random coil(%)
3.0	58.86 ± 1.00^{f}	7.60 ± 0.08^{a}	10.76 ± 0.16^{a}	23.62 ± 0.34^{a}	44.67 ± 0.38^{g}	9.61 ± 0.07^{a}	14.54 ± 0.22^{c}	24.87 ± 0.26^{a}
4.0	39.68 ± 0.27^{c}	10.38 ± 0.11^{c}	16.53 ± 0.28^{c}	34.62 ± 0.94^{f}	31.42 ± 0.53^{e}	12.59 ± 0.52^{b}	13.70 ± 0.96^{b}	42.53 ± 0.35^{e}
5.0	16.77 ± 0.22^{a}	36.88 ± 0.66^{e}	19.75 ± 0.37^{e}	32.66 ± 0.58^{e}	6.41 ± 0.64^{a}	53.30 ± 0.38^{f}	16.46 ± 0.12^{e}	28.63 ± 0.11^{b}
6.0	20.94 ± 0.86^{b}	27.44 ± 0.04^{d}	18.24 ± 0.16^{d}	34.90 ± 0.11^{f}	24.12 ± 0.31^{c}	20.78 ± 0.69^{d}	15.58 ± 0.11^{d}	43.14 ± 0.85^{e}
7.0	20.39 ± 0.47^{b}	27.32 ± 0.20^{d}	17.91 ± 0.49^{d}	36.26 ± 0.14^{g}	18.13 ± 0.33^{b}	33.32 ± 0.80^{e}	18.85 ± 0.09^{f}	35.25 ± 0.46^{c}
8.0	45.00 ± 0.70^{d}	9.16 ± 0.25^{b}	15.84 ± 0.50^{b}	30.04 ± 0.31^{c}	25.74 ± 0.67^{d}	17.88 ± 0.72^{c}	15.44 ± 0.56^{d}	41.06 ± 0.69^{d}
9.0	44.95 ± 0.09^{d}	8.96 ± 0.59^{b}	15.71 ± 0.21^{b}	31.58 ± 0.02^{d}	25.16 ± 0.27^{d}	18.27 ± 0.26^{c}	15.72 ± 0.09^{de}	40.37 ± 0.61^{d}
10.0	55.45 ± 0.52^{e}	7.98 ± 0.33^{a}	11.19 ± 0.25^{a}	25.59 ± 0.24^{b}	42.15 ± 0.99^{f}	8.83 ± 0.08^{a}	10.49 ± 0.41^{a}	44.16 ± 0.11^{f}

Different letters in the same column indicate significant differences between the data ($P < 0.05$).

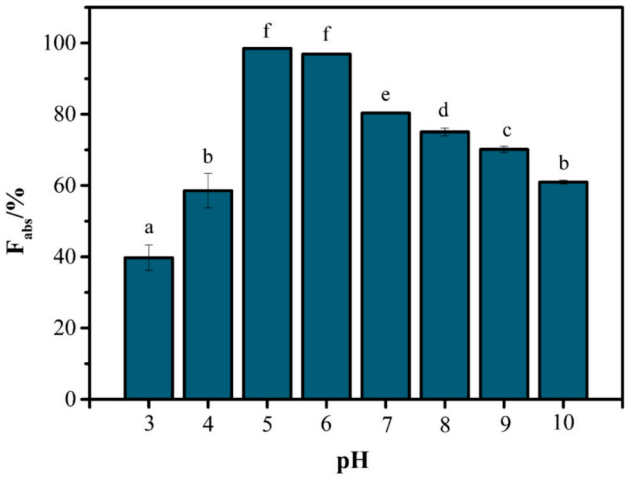

Fig. 5. Interface adsorbed protein content of TPI emulsions at different pH (3.0–10.0).

3.3.3. SDS-PAGE

The SDS-PAGE was used to reveal the composition of the interfacial proteins of the TPI emulsions. As is shown in Fig. 6, interface-adsorbed protein mainly consists of a myosin-heavy chain with molecular weights of 200 kDa and actin with a molecular weight of 43.3 kDa, suggesting water-insoluble proteins are more oleophilic. At pH 5.0, only a small amount of tropomyosin existed in the aqueous phase. This may be due to the following facts: the TPI with low solubility has a large aggregate and weak interaction with water; the aggregate is close to the surface of the oil droplet. However, at pH 5.0, the molecular structure of TPI does not dissociate and unfold, leading to no interfacial film formed in the O/W interface, resulting in poor emulsion stability (Fig. 3). At pH 7.0, the protein effectively surrounds the lipid particles as the solubility of the protein increases (Table S1). Due to insufficient electrostatic repulsion between droplets, partial phase separation occurs during the storage process (Fig. 2). No significant difference was determined in protein types between the adsorbed and non-adsorbed layers under other pH modifications. Myosin light chain, water-soluble protein mainly in the aqueous phase. The content and thickness of interfacial proteins affect the physicochemical properties of emulsion. Under the alkaline condition (pH 10.0), the partially unfolded protein structure exposes the hydrophobic zoom, disulfide bond, and reactive amino acids, resulting in a high viscoelastic interface to resist droplet aggregation.

3.4. Correlation analysis between secondary structure and emulsion stability

The relationship between secondary structure and emulsion stability is presented in Table 2. The secondary structure of TPI without high-pressure homogenization treatment was significantly correlated with surface electrostatic charge and emulsion stability under the influence of pH ($P < 0.05$). Among them, surface electrostatic charge and emulsion stability presented a very significant positive correlation with α-helix ($P < 0.01$) and a negative correlation with β-sheet, β-turn, and random coil ($P < 0.05$). After high-pressure homogenization, emulsion stability was positively correlated with the α-helix ($P < 0.05$) and negatively correlated with the β-sheet ($P < 0.05$). The comparison of samples before and after homogenization indicated that pH has a more significant impact on the secondary structure than the homogenization treatment itself in enhancing emulsion stability. Thus, pH regulation can alter the surface electrostatic charge of proteins. The exposure of charged groups affects the folding of proteins, further affects the secondary structure of proteins, and finally improves the emulsion stability. Therefore, pH regulation can change the electrostatic charge on the protein surface, and homogenization can induce the protein structure to unfold. Under extreme acid-base conditions, an increase in charged groups affects the folding of proteins, further affects the protein's structure, and finally improves the emulsion stability. The α-helix depends on hydrogen bonds and is more stable than β-turn (Wu, Xu, Wu, Xiong, & Wang, 2020). Therefore, the increase in α-helix content means that proteins form hydrogen bonds with water molecules in a water-based environment, which enhances the emulsifying ability of proteins and is conducive to emulsion stability.

4. Conclusions

This study showed that pH affects TPI emulsion stability by altering the structure of adsorbed proteins at the O/W interface. As pH moves away from the protein *pI*, the TPI presents more surface electrostatic charge, which affects protein folding and significantly increases the content of α-helix in the protein secondary structure (α-helix content showed a high positive correlation with TPI emulsions stability). These changes in the secondary structure of interface protein improve protein solubility and emulsifying properties, ultimately leading to increased emulsion stability. This study revealed the association between the secondary structure of interfacial proteins and TPI emulsion stability under different pH to provide theoretical guidance for subsequent methods to enhance the emulsion stability. Developing novel and stable TPI emulsions for the food industry is highly beneficial.

CRediT authorship contribution statement

Qingguan Liu: Writing – original draft, Investigation, Funding acquisition. **Ailin Chen:** Methodology, Investigation, Formal analysis. **Pengzhi Hong:** Software, Methodology, Formal analysis. **Chunxia Zhou:** Writing – review & editing, Supervision, Project administration. **Xiang Li:** Methodology, Formal analysis. **Mengya Xie:** Methodology, Formal analysis.

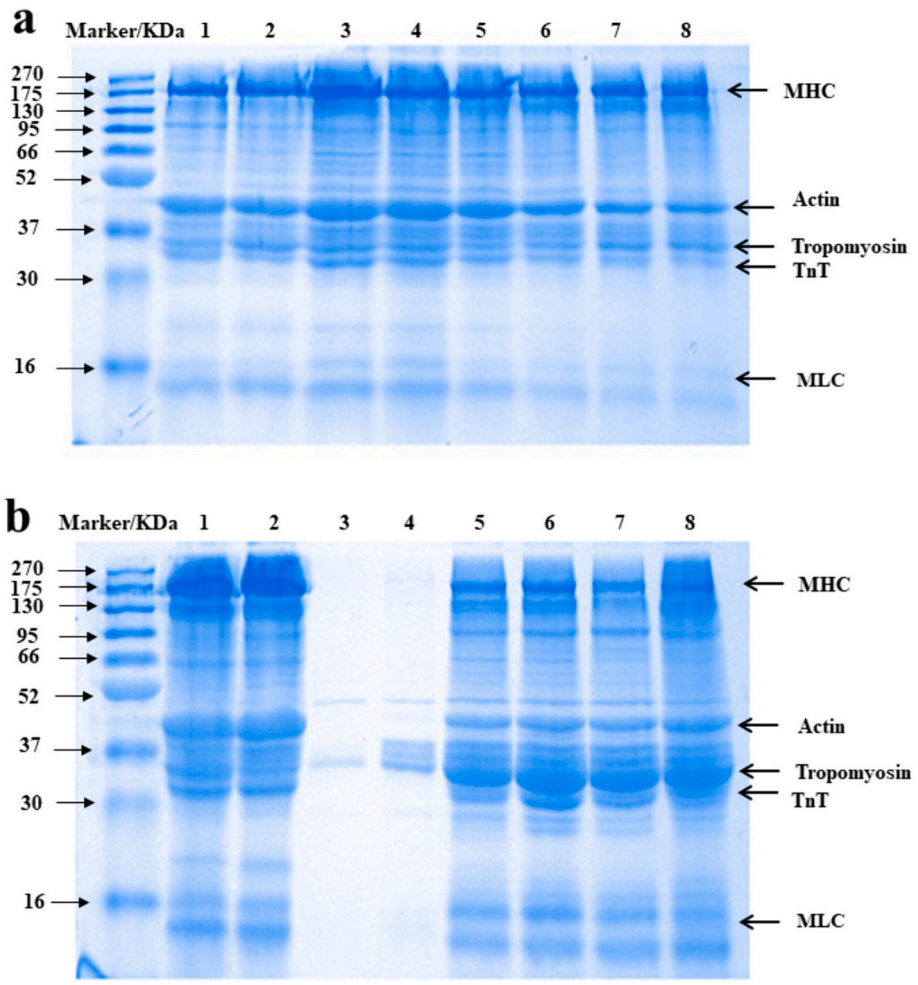

Fig. 6. SDS-PAGE profiles of adsorbed (a) and non-adsorbed (b) proteins (Lanes 1–8 represent pH 3.0–10.0).

Table 2
Correlation analysis between secondary structure and emulsion stability.

Items	Before homogenization				After homogenization			
	α-helix (%)	β-sheet (%)	β-turn (%)	Random coil (%)	α-helix (%)	β-sheet (%)	β-turn (%)	Random coil (%)
1	0.905**	−0.827*	−0.942**	−0.798*	0.859**	−0.765*	−0.478	−0.031
2	0.901**	−0.822*	−0.955**	−0.788*	0.949**	−0.848**	−0.534	−0.06
3	−0.669	0.803*	0.651	0.301	−0.777*	0.901**	0.331	−0.414
4	0.873**	−0.803*	−0.878**	−0.735*	0.796*	−0.727*	−0.566	0.061

Items 1 represent the surface electrostatic charge before homogenization; Items 2 represent the surface electrostatic charge after homogenization; Items 3 represent particle size; Items 4 represent the stability coefficient; * indicates $P < 0.05$; ** indicates $P < 0.01$.

Declaration of competing interest

The authors declare that they have no known competing financial interests or personal relationships that could have appeared to influence the work reported in this paper.

Data availability

Data will be made available on request.

Acknowledgments

This work was supported by the Zhanjiang Science and Technology Program Project (2022A05037), and Guangdong Modern Agricultural Industrial Technology System Innovation Team Building Project (2023KJ150).

Appendix A. Supplementary data

Supplementary data to this article can be found online at https://doi.org/10.1016/j.fochx.2024.101841.

References

Al-Saadi, J. M. S., & Deeth, H. C. (2011). Preparation and functional properties of protein coprecipitate from sheep milk. *International Journal of Dairy Technology, 64*(4), 461–466.

Brenner, T., Johannsson, R., & Nicolai, T. (2009). Characterisation and thermo-reversible gelation of cod muscle protein isolates. *Food Chemistry, 115*(1), 26–31.

Chalamaiah, M., Kumar, B. D., Hemalatha, R., & Jyothirmayi, T. (2012). Fish protein hydrolysates: Proximate composition, amino acid composition, antioxidant activities and applications: A review. *Food Chemistry, 135*(4), 3020–3038.
Chen, N., Nicolai, T., Chassenieux, C., & Wang, Y. (2020). pH and ionic strength responsive core-shell protein microgels fabricated via simple coacervation of soy globulins. *Food Hydrocolloids, 105*, Article 105853.
Chen, X., Zhou, R., Xu, X., Zhou, G., & Liu, D. (2017). Structural modification by high-pressure homogenization for improved functional properties of freeze-dried myofibrillar proteins powder. *Food Research International, 100*(pt.1), 193.
Drapala, K. P., Mulvihill, D. M., & O'Mahony, J. A. (2018). A review of the analytical approaches used for studying the structure, interactions and stability of emulsions in nutritional beverage systems. *Food Structure, 16*, 27–42.
Du, C., Cai, Y., Liu, T., Huang, L., Long, Z., Zhao, M., & Zhao, Q. (2020). Physicochemical, interfacial and emulsifying properties of insoluble soy peptide aggregate: Effect of homogenization and alkaline-treatment. *Food Hydrocolloids, 109*, Article 106125.
Egerton, S., Culloty, S., Whooley, J., Stanton, C., & Ross, R. P. (2018). Characterization of protein hydrolysates from blue whiting (*Micromesistius poutassou*) and their application in beverage fortification. *Food Chemistry, 245*, 698–706.
FAO. (2024). *The state of world fisheries and aquaculture 2024. Blue Transformation in action. Rome.* https://doi.org/10.4060/cd0683en
Felix, M., Romero, A., & Guerrero, A. (2017). Influence of pH and xanthan gum on long-term stability of crayfish-based emulsions. *Food Hydrocolloids, 72*, 372–380.
Garti, N., Slavin, Y., & Aserin, A. (1999). Portulaca oleracea gum and casein interactions and emulsion stability. *Food Hydrocolloids, 13*(2), 127–138.
Greenfield, N. J. (2006). Using circular dichroism collected as a function of temperature to determine the thermodynamics of protein unfolding and binding interactions. *Nature Protocols, 1*(6), 2527.
Hemung, B. O., Benjakul, S., & Yongsawatdigul, J. (2013). pH-dependent characteristics of gel-like emulsion stabilized by threadfin bream sarcoplasmic proteins. *Food Hydrocolloids, 30*(1), 315–322.
Hu, J., Yu, B., Yuan, C., Tao, H., Wu, Z., Dong, D., Lu, Y., Zhang, Z., Cao, Y., Zhao, H., Cheng, Y., & Cui, B. (2023). Influence of heat treatment before and/or after high-pressure homogenization on the structure and emulsification properties of soybean protein isolate. *International Journal of Biological Macromolecules, 253*, Article 127411.
Hu, M., Xie, F., Zhang, S., Li, Y., & Qi, B. (2020). Homogenization pressure and soybean protein concentration impact the stability of perilla oil nanoemulsions. *Food Hydrocolloids, 101*, Article 105575.
Huang, X., Cui, Y., Shi, L., Yang, S., Qiu, X., Hao, G., Zhao, Y., Liu, S., Liu, Z., Weng, W., & Ren, Z. (2023). Structural properties and emulsification of myofibrillar proteins from hairtail (*Trichiurus haumela*) at different salt ions. *International Journal of Biological Macromolecules, 253*, Article 127598.
Huang, X., Liu, Q., Wang, P., Song, C., Ma, H., Hong, P., & Zhou, C. (2024). Tapioca starch improves the quality of Virgatus nemipterus surimi gel by enhancing molecular interaction in the gel system. *Foods, 13*, 169.
Jiang, J., Chen, J., & Xiong, Y. L. (2009). Structural and emulsifying properties of soy protein isolate subjected to acid and alkaline pH-shifting processes. *Journal of Agricultural and Food Chemistry, 57*(16), 7576–7583.
Kato, A., Komatsu, K., Fujimoto, K., & Kobayashi, K. (1985). Relationship between surface functional properties and flexibility of proteins detected by the protease susceptibility. *Journal of Agricultural and Food Chemistry, 33*(5), 931–934.
Kristinsson, H. G., & Hultin, H. O. (2004). Changes in trout hemoglobin conformations and solubility after exposure to acid and alkali pH. *Journal of Agricultural and Food Chemistry, 52*(11), 3633–3643.
Laemmli, U. K. (1970). Cleavage of structural proteins during the assembly of the head of bacteriophage T4. *Nature, 227*(5259), 680–685.
Langevin, D. (2014). Surface shear rheology of monolayers at the surface of water. *Advances in Colloid and Interface Science, 207*(pp), 121–130.
Li, K., Fu, L., Zhao, Y. Y., Xue, S. W., Wang, P., Xu, X. L., & Bai, Y. H. (2020). Use of high-intensity ultrasound to improve emulsifying properties of chicken myofibrillar protein and enhance the rheological properties and stability of the emulsion. *Food Hydrocolloids, 98*, Article 105275.
Li, Q., Wang, Z., Dai, C., Wang, Y., Chen, W., Ju, X., & He, R. (2019). Physical stability and microstructure of rapeseed protein isolate/gum Arabic stabilized emulsions at alkaline pH. *Food Hydrocolloids, 88*, 50–57.
Li, R., True, A. D., Sha, L., & Xiong, Y. L. (2024). Structural modification of oat protein by thermosonication combined with high pressure for O/W emulsion and model salad dressing production. *International Journal of Biological Macromolecules, 255*, Article 128109.
Li, X., Hong, P., Xie, M., Wang, Y., Liu, Q., & Zhou, C. (2024). Formation of hydrophilic co-assemblies with improved functional properties between tilapia protein isolate and sodium caseinate. *Food Hydrocolloids, 153*, Article 110016.
Li, Y., Li, M., Qi, Y., Zheng, L., Wu, C., Wang, Z., & Teng, F. (2020). Preparation and digestibility of fish oil nanoemulsions stabilized by soybean protein isolate-phosphatidylcholine. *Food Hydrocolloids, 100*, Article 105310.
Liu, Q., Sun, Y., Cheng, J., Zhang, X., & Guo, M. (2022). Changes in conformation and functionality of whey proteins induced by the interactions with soy isoflavones. *LWT - Food Science and Technology, 163*, Article 113555.
Liu, Q., Tan, L., Hong, P., Liu, H., & Zhou, C. (2024). Tilapia-soybean protein co-precipitates: Focus on physicochemical properties, nutritional quality, and proteomics profile. *Food Chemistry: X, 21*, Article 101179.
Ma, W., Wang, J., Wu, D., Xu, X., Wu, C., & Du, M. (2020). Physicochemical properties and oil/water interfacial adsorption behavior of cod proteins as affected by high-pressure homogenization. *Food Hydrocolloids, 100*, Article 105429.
Ma, W., Wang, J., Xu, X., Qin, L., Wu, C., & Du, M. (2019). Ultrasound treatment improved the physicochemical characteristics of cod protein and enhanced the stability of oil-in-water emulsion. *Food Research International, 121*, 247–256.
Mozafarpour, R., Koocheki, A., Milani, E., & Varidi, M. (2019). Extruded soy protein as a novel emulsifier: Structure, interfacial activity and emulsifying property. *Food Hydrocolloids, 93*, 361–373.
Nilsson, L., & Bergenstahl, B. (2006). Adsorption of hydrophobically modified starch at oil/water interfaces during emulsification. *Langmuir, 22*(21), 8770–8776.
Pearce, K. N., & Kinsella, J. E. (1978). Emulsifying properties of proteins: Evaluation of a turbidimetric technique. *Journal of Agricultural and Food Chemistry, 26*(3), 716–723.
Surh, J., Decker, E. A., & McClements, D. J. (2006). Influence of pH and pectin type on properties and stability of sodium-caseinate stabilized oil-in-water emulsions. *Food Hydrocolloids, 20*(5), 607–618.
Tan, L., Hong, P. Z., Yang, P., Zhou, C. X., Xiao, D. H., & Zhong, T. J. (2019). Correlation between the water solubility and secondary structure of Tilapia-soybean protein co-precipitates. *Molecules, 24*(23), 4337.
Tian, Y., Zhang, Z., Zhang, P., Taha, A., & Pan, S. (2020). The role of conformational state of pH-shifted β-conglycinin on the oil/water interfacial properties and emulsifying capacities. *Food Hydrocolloids, 108*, Article 105990.
Tomczynska-Mleko, M., Sikorska, E., Wesolowska-TroAnowska, M., Kamysz, E., Ozimek, L., Kowaluk, G., & Gustaw, W. (2014). Changes of secondary structure and surface tension of whey protein isolate dispersions upon pH and temperature. *Czech Journal of Food Sciences, 32*, 82–89.
Van, D. C., Keuchenius, C., De, V. J. H. M., De, B. J., & Aiking, H. (2018). Unsustainable dietary habits of specific subgroups require dedicated transition strategies: Evidence from the Netherlands. *Food Policy, 79*, 44–57.
Wang, J., Lin, M., Shi, L., Zhao, Y., Liu, S., Liu, Z., & Ren, Z. (2024). Characteristics and stabilization of Pickering emulsions constructed using myosin from bighead carp (*Aristichthys nobilis*). *Food Chemistry, 456*, Article 140033.
Wihodo, M., & Moraru, C. I. (2013). Physical and chemical methods used to enhance the structure and mechanical properties of protein films: A review. *Journal of Food Engineering, 114*(3), 292–302.
Wu, J., Xu, F., Wu, Y., Xiong, W., & Wang, L. (2020). Characterization and analysis of rapeseed protein isolate stabilized O/W emulsion under pH and ionic stress. *Journal of the Science of Food and Agriculture, 100*(13), 4734–4744.
Wu, Y., Wu, Y., Xiang, H., Chen, S., Zhao, Y., Cai, Q., & Wang, Y. (2024). Emulsification properties and oil-water interface properties of l-lysine-assisted ultrasonic treatment in sea bass myofibrillar proteins: Influenced by the conformation of interfacial proteins. *Food Hydrocolloids, 147*, Article 109405.
Xi, C., Kang, N., Zhao, C., Liu, Y., Sun, Z., & Zhang, T. (2020). Effects of pH and different sugars on the structures and emulsification properties of whey protein isolate-sugar conjugates. *Food Bioscience, 33*, Article 100507.
Xia, X., Kong, B., Xiong, Y., & Ren, Y. (2010). Decreased gelling and emulsifying properties of myofibrillar protein from repeatedly frozen-thawed porcine longissimus muscle are due to protein denaturation and susceptibility to aggregation. *Meat Science, 85*(3), 481–486.
Xie, M., Zhou, C., Li, X., Ma, H., Liu, Q., & Hong, P. (2024). Preparation and characterization of tilapia protein isolate – Hyaluronic acid complexes using a pH-driven method for improving the stability of tilapia protein isolate emulsion. *Food Chemistry, 445*, Article 138703.
Yan, S., Xu, J., Zhang, S., & Li, Y. (2021). Effects of flexibility and surface hydrophobicity on emulsifying properties: Ultrasound-treated soybean protein isolate. *LWT - Food Science and Technology, 142*, Article 110881.
Yerramilli, M., & Ghosh, S. (2017). Long-term stability of sodium caseinate-stabilized nanoemulsions. *Journal of Food Science and Technology-Mysore, 54*(1), 82–92.
Zhang, J., Liu, Q., Chen, Q., Sun, F., Liu, H., & Kong, B. (2022). Synergistic modification of pea protein structure using high-intensity ultrasound and pH-shifting technology to improve solubility and emulsification. *Ultrasonics Sonochemistry, 88*, Article 106099.
Zhang, M., Zhou, L., Yang, F., Yao, J., Ma, Y., & Liu, J. (2022). Construction of high internal phase Pickering emulsions stabilized by bamboo fungus protein gels with the effect of pH. *Food Chemistry, 369*, Article 130954.
Zhao, X., Bai, Y., Xing, T., Xu, X.-L., & Zhou, G. (2018). Use of an isoelectric solubilization/precipitation process to modify the functional properties of PSE (pale, soft, exudative)-like chicken meat protein: A mechanistic approach. *Food Chemistry, 248*, 201–209.
Zhu, X., Li, L., Li, S., Ning, C., & Zhou, C. (2019). L-arginine/L-lysine improves emulsion stability of chicken sausage by increasing electrostatic repulsion of emulsion droplet and decreasing the interfacial tension of soybean oil-water. *Food Hydrocolloids, 89*, 492–502.